Journal of Metals, Materials and Minerals. Vol. 12 No. 2 pp. 81-87, 2003.

Electrospinning Process of Molten Polypropylene in Vacuum

Ratthapol RANGKUPAN[1] and Darrell H. RENEKER[2]

[1]Metallurgy and Materials Science Research Institute, Chulalongkorn University, Bangkok, Thailand
[2]Maurice Morton Institute of Polymer Science, University of Akron, Akron, OH, USA

ABSTRACT

Very fine polypropylene (PP) fibers were made from molten PP in vacuum using an electrospinning process. Under the influence of a modest external electric field, a droplet of PP melt was pulled out, trailed by a jet that became thin and soon broke. When the electric field strength was increased, a steady charged jet flew toward a collector. Jets solidified to form fibers either in flight or after reaching the collector. The semi-angle of the Taylor cone from which the jet emerged was about 37.5 ± 2 °. The diameters of the fibers ranged from 300 nanometers to 30 microns. Scanning electron micrographs showed a variety of fiber morphologies, including coils indicating that the charged jet developed an electrically driven bending instability.

INTRODUCTION

The electrospinning process utilizes an electrostatic force to destabilize a surface of a polymer liquid droplet, creating a charged jet that elongates and solidifies to form an electrospun fiber. (Doshi, *et al.* 1993; and Doshi, 1994). Electrospinning provides an attractive and relatively easy route to produce nanofibers and thicker fibers. Advantages over the conventional spinning of fine fibers, such as a conjugated spinning method, include a simple apparatus, a compact spinning station, a wide range of materials that can be used and, best of all, its capability of producing fibers with very small diameters.

The diameter of electrospun fibers are typically in the range of tens to a few hundreds of nanometers for solution electrospinning and in the range of hundreds of nanometer to a few micrometers for fibers electrospun from molten polymers. (Doshi, *et al.* 1993; Doshi, 1994; Chun, 1995; Koombhongse, 2001; and Rangkupan, 2002). For comparison, the diameters of conventional textile fibers made by typical spinning processes are about 10 to 20 micrometers or more. The diameter of electrospun fibers is one to two orders of magnitude smaller than that of conventional fibers. Because of its smaller diameter, an electrospun fiber has a higher specific surface area than a conventional textile fiber. This feature is attractive to many applications that require a high surface area or high specific surface area. Figure 1 shows a plot of a specific surface area as a function of fiber diameter, assuming that the fiber has a circular cross section and a density of 1 gram per cm^3. The arrow indicates a typical range of diameter for electrospun fibers.

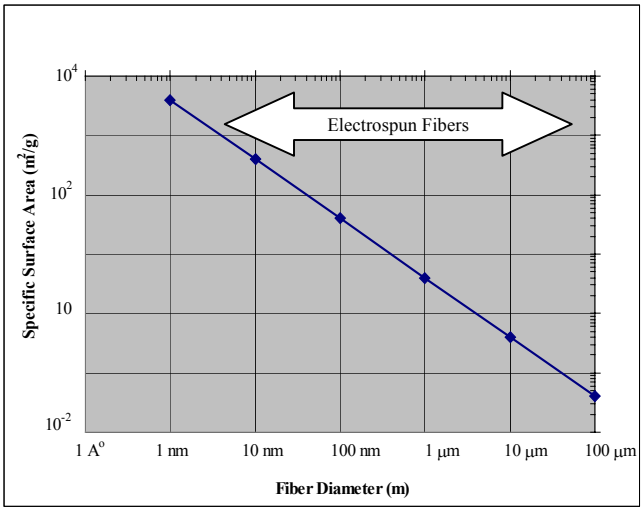

Figure 1 Specific surface area as a fucntion of fiber diameter. Circular cross sections and a density of 1 g/cm^3 were assumed. Arrow indicates the typical range of diameters of fibers electrospun from polymer solutions and melts.

Several applications for electrospun fibers are under development including filtration of

submicron particles in separation industries, artificial blood vessels, sutures, wound dressings, controlled drug released and tissue engineering scaffolds for biomedical applications, controlling application of pesticides in agriculture, protective clothing against chemical warfare agents, nanotube construction, optical sensors, nanofiber solar cells, nanocomposites, and contruction of solar sails (Koombhongse, 2001; Rangkupan, 2002; Liu, *et al.* 2002; Schreuder-Gibson, *et al.* 2002; Wang, *et al.* 2002; Lennhoff, *et al.* 2002; and Whithe, *et al.* 2002).

With few exceptions, (Chun, 1995; and Larrando, *et al.* 1981) studies of the electrospinning process and the applications for electrospun nanofibers were made by electrospinning a polymer solution. It is presently more difficult to electrospin fiber from a polymer melt than from a polymer solution because of the higher viscosity and lower electrical conductivity of molten polymers (Rangkupan, 2002). Moreover, the diameter of a melt-electrospun fiber, which can be in the range of tens of micron, is much larger than the diameter of a solution-electropun fiber, making fibers with a range of diameters that is achieved with conventional apparatus.

Melt–electrospinning eliminates the cost associated with the removal and recovery of the solvents, and any health risks associated with solvents. Melt-electrospinning complements the solution-electrospinning for polymers which are difficult to dissolve. It is clear that further study about the melt-electrospinning process, from both scientific and engineering standpoints can produce valuable information.

The objectives for this study were to produce sub-micron fibers from molten polypropylene and to prove the concept of producing a very fine fiber in space using electrospinning process. A vacuum system simulates a space environment, and takes advantage of the much higher electrical break down strength of a vacuum compared to air. This enables us to obtain higher electric fields which exerts larger electrical forces on the fluid jet.

MATERIALS AND EXPERIMENTAL SET UP

Material

Polypropylene (PP) used in this study was obtained from Aldrich and used as received. The molecular weight was 190,000 with a melt flow index (MI) of 35 g per10 min, at 200^{o}C and 10 kg. Load (Sigma-Aldrich).

Experimental apparatus

Figure 2 shows a schematic diagram of a typical appartus used in this study. PP pellets were loaded into a spinneret, typically a copper cup with a 1.5 mm hole on the side, and melted with a radiant heater at the temperature about 250 to 300^{o}C. Charges were supplied by a copper wire connected to the spinneret. The wire was connected to either a positive or negative high voltage power supply outside a vacuum chamber through an electrical feed-through. The high voltage power supply used was a dual polarity high voltage power supply model D-ES30PN/M692 by Gamma High Voltage Research. The input voltages were read from analog voltage meters on the power supply. A collector plate, made of an aluminum sheet was placed 20 to 150 mm away from the spinneret and maintained at a high electrical potential. The electric field strength between the spinneret and the collector was varied from 100 to 3000 kV/m.

The behavior of a charged jet during the electrospinning process was followed by a video camera, connected to a 12.5-75 mm zoom lens, with and without a 2X close up lens. An observation window was located at the front panel of a vacuum chamber. Multiple halogen lamps were positioned inside the vacuum chamber at strategic locations to illuminate the jet.

Electrical current carried by the molten jet was monitored by a nanoampere meter, which was maintained at the potential of the spinneret. A similar nanoampere meter maintained at the potential of the collector, measured the current flowing to the collector. This arrangement of two ampmeters monitored the jet current and provided an indication of leakage currents if they were present.

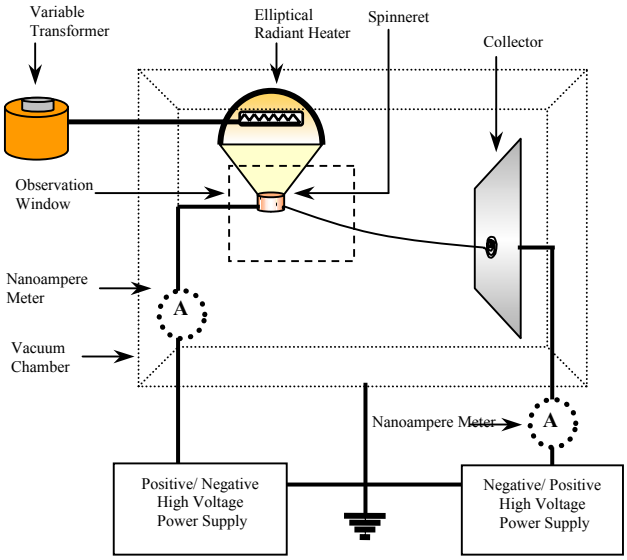

Figure 2 Schematic diagram of apparatus for electrospinning of molten polymers in a vacuum

Figure 3 Image of apparatus for electrospinning of polymer melts in a vacuum as outline in figure 2. The radiant heat source is in the metal box at the top center. The nanofibers collected on the wrinkled aluminum sheet are visible on the right hand side of the figure. The spinneret is immediately below the radiant heater.

RESULTS AND DISCUSSION.

The electrospinning process of molten polymers can be divided into 3 steps: initiation of the charged jet, elongation of the jet, and solidification of the jet.

Initiation of a molten charged jet in vacuum

When the external electric field was applied to a molten hemispherical droplet, excess charges, such as mobile ions from impurities, with the polarity of the electrode, migrate to the surface of the droplet of molten polymer. A repulsive force, from the Coulombic interactions between the ions, tends to increase the surface area, while the surface tension tends to minimize the surface area. At a sufficiently high field, the surface tension was overwhelmed by Coulombic interaction and the surface area grew by deformation of the shape of the droplet from hemispherical to conical.

A further increase in the electric field strength caused the droplet to deform more, creating a cone with a sharper tip. At the critical field strength, at which the electrical forces equal the surface tension, the droplet assumed the shape of the Taylor cone. Above the critical field strength, the electrical forces overcame both surface tension and the viscous forces within the melt, a tiny droplet of molten polymer was pulled out of the tip of the cone. The droplet was trailed by a jet that became thin and often broke. When the electric field strength was again increased, a steady charged jet formed and flew toward the collector. Multiple charged jets were created occasionally at high field strength. At a melt temperature of 250^{o}C, the critical electric field strength was about 200-400 kV/m, and a steady charged jet was formed above this field strength.

The mobile charges in the melts were believed to come from small concentrations of ionic impurities, from sources such as monomer residues, other chemicals used during a post-polymerization step, contamination during handling of polymer and moisture uptake. Charges may also come from other charging mechanisms, such as an ion transfer between an electrode and the melt, and by ionization of residual gases in the vacuum chamber (Cross, 1987).

Figure 4 shows the initiation of a charged jet of molten PP electrospun at 300^{o}C, in an electric field of 200 kV/m. After the electric field was applied for about 60 seconds, a droplet of molten polymer hanging from the orifice started to deform from a semi-spherical to an elongated droplet. After the critical shape was formed at t = 0 s, ejection of the charged jet occurred at t = 0.20 s. The steady charged jet was formed at about t = 2 s. For comparison, for a sessile droplet of an aqueous solution of 6% poly(ethylene oxide) electrospun in an electric field of 146 kV/m, the critical shape formed at t= 0.77 s and charged jet ejection occurred at t = 0.83 s.

(Koombhongse, 2001). The times involved in the critical shape formation and steady charged jet ejection in the melt were considerably longer than those in the solution. The longer time is associated with a slower charge migration rate in polymer melts, a lower charge concentration at the surface and a higher surface tension in the melt.

From figure 4, at t= 0 s., the semi-angle of the cone at the critical point observed from the experiment, α_{EXP}, was about 37.5 ± 2°. This value was closer to the prediction of a semi-angle of the cone at the critical point by Yarin, α_Y, at 33.5° than the prediction of a semi-angle of the Taylor cone, α_T, at 49.9° (Yarin, *et al.* 2001; and Taylor, 1964). Because the exact moment at which the theoretical equilibrium condition was satisfied was difficult to pinpoint from visual observation, the point at which the Taylor cone was formed was determined by analyzing numerous video images.

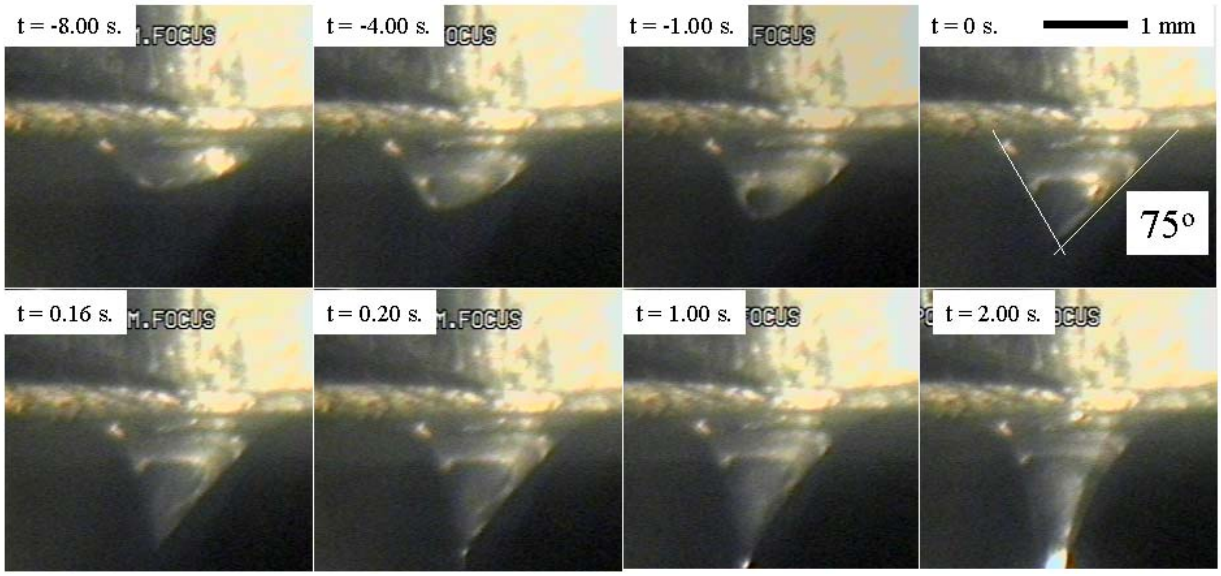

Figure 4 Video images of a formation of the critical shape and a charged jet ejection from a droplet of molten PP electrospun at 300°C, in a 200 kV/m electric field.

Elongation of a molten charged jet in vacuum

The Coulombic repulsion among surface charges on the jet is the dominant force that causes the segment of the jet to elongate, and to eventually cause a bending instability. As the jet segment elongates, its diameter decreases. The elongation of the jet continue as long as the electrical forces can overcome the surface tension and viscoelastic forces, even the presence of the bending instability.

Experimental observations showed that after a charged jet of molten polymer was ejected from the droplet, the jet often flew toward a collector as a straight jet without developing any bending instability. Occasionally, the jet coiled and oscillated back and forth in a motion resembling the faster electrically-driven bending instability observed in a solution electrospinning. Images from an ordinary video camera, recorded at 30 frames per second, were unable to resolved the jet path in detail, and use of a high frame rate camera was also unrewarding because of constraints imposed by the vacuum chamber.

Scanning electron microscope images of fibers electrospun in vacuum showed coils indicated that the molten charged jet developed the electrically-driven bending instability. Rangkupan reported the formation of an electrically-driven bending instability of a molten charged-jet of poly(ε-caprolactone) electrospun in air (Rangkupan, 2002). The behavior of a molten charged jet in vacuum was expected to be similar to the behavior of a molten charged jet electrospun in air, since the electrospinning process in vacuum and in air were essentially identical, with the main difference lying in the solidification of the charged jets. Also the viscous forces of the air were small since the velocity was low.

Solidification of a charged jet of molten polymers

Solidification of the charged jet is often the termination step of the electrospinning process. After a molten charged jet solidifies into a strong fiber, elongation can no longer occur. The solidification process in solution electrospinning takes place via evaporation of solvent. The solidification of the fibers in the melt electrospinning process, however, takes place through a radiation of thermal energy from the jet to its cooler surroundings.

In a vacuum, heat dissipation of molten charged jet took place in two stages. The first stage occurred as soon as the jet emerged from the spinneret and flew toward the collector. Heat was removed mainly through the radiation process. Any thermal energy remaining after the jet reached the collector was removed by conduction to the collector.

Diameter of electrospun fibers

Fibers electrospun from molten polymers were often collected in a small area. When the electrospinning was done in an axisymmetric electric field, such as the field in a point and plate geometry, a fiber mat was collected into a small circular area that grew larger with time. The center of the mat was near the point at which a line perpendicular to the collector projected to the spinneret. When the electric field was not symmetric, the shape of collected fiber mats deviated from a circular shape and was difficult to predict.

The diameter of electrospun polypropylene fibers was in the range of 300 nm to 30 μm. The fiber diameter tended to decrease as processing temperature increased, as the distance between the spinneret and collector increased, and as the electric field strength increased. The diameter of fiber segments had large variation along the length of the fiber, often showing multi-modal histograms of fiber diameter. The term 'fiber segment' was used because different segments of a long single fiber were photographed in the same image. The diameter variation of the fiber segment was affected by: (i) the mass flow rate of the molten polymer to the site where the jet ejection occurred was lower than the fiber formation rate, thereby starving the segment and reducing its diameter, (ii) the elongation of each segments of the charged jet was not uniform, (iii) charge density in the fiber was not uniform, (iv) different segments of the charged jet solidified at different rate, and (v) a fluctuation in electrical field strength caused by corona discharge or other reasons which could be controlled .

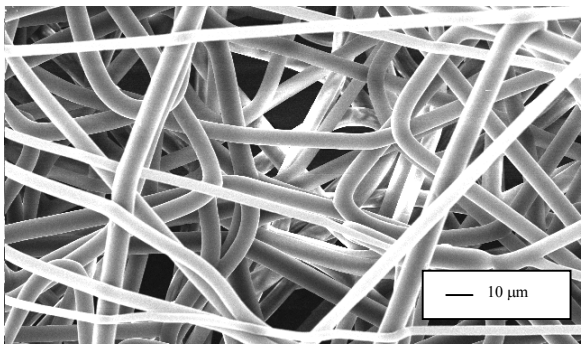

Figure 5 SEM image of PP fibers electrospun in vacuum

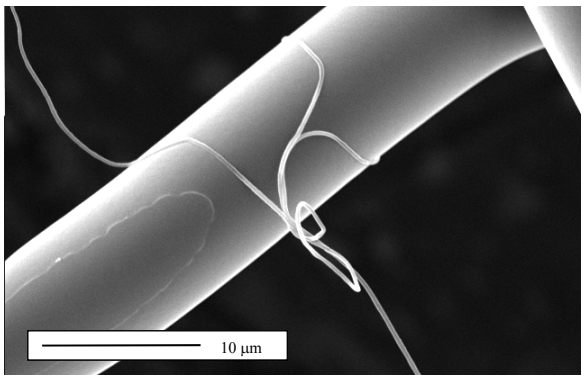

Figure 6 SEM image of electrospun polypropylene fiber. It shows PP nanofiber, with a diameter of about 300 nanometers, wrapped around a bigger electrospun PP fiber, which had a diameter in the range of a very fine textile fiber.

Morphology of electrospun fibers

The morphology of electrospun fibers was examined using scanning electron microscopy and optical microscopy. Figure 5 shows an image of regular PP fibers electrospun in vacuum. The fibers were fully solidified before they were collected and had a smooth texture. Figure 6 shows PP nanofiber, with a diameter of about 300 nanometers, wrapped around a bigger electrospun PP fiber, which had a diameter in the range of a very fine textile fiber.

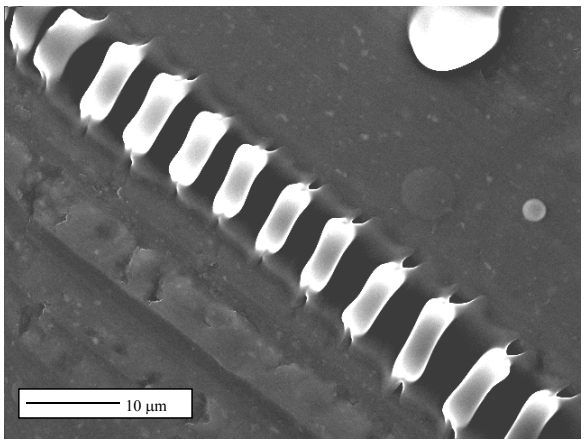

Figure 7 SEM image of a PP ribbon with instability waves on the ribbon. The ribbon was collected before the wave could grow and stretch out to form a flat ribbon.

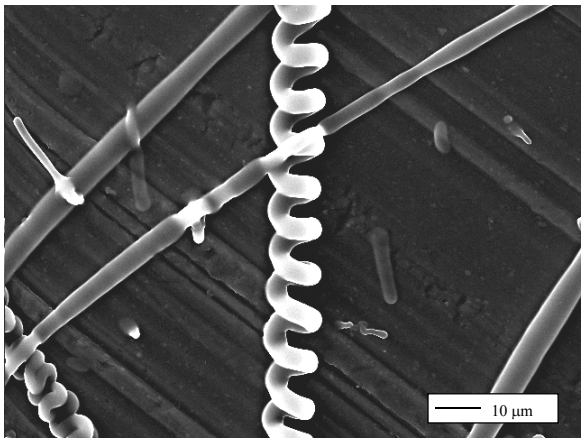

Figure 8 SEM image of electrospun PP fibers. A spring-like morphology in a main fiber (running from top to bottom in the middle) was an indication of the development of the electrically-driven bending instability in a small scale.

Figure 7 shows a SEM image of a PP ribbon with instability waves on the ribbon. The ribbon was collected before the wave could grow and stretch out to form a flat ribbon. Figure 8 shows a spring-like morphology in a fiber running from top to bottom in the middle, which is an indication of the occurrence of an electrically-driven bending instability in the electrospinning of a jet of molten polypropylene. Other morphologies observed included coiled and bent fibers. Depending on the path of the collected fibers and the details of the bending instability, different segments of the same fiber could exhibit different morphologies.

SUMMARY

Polypropylene was successfully electrospun into fine fibers with a diameters in the range of 300 nm to 30 μm with a large fiber diameter variation. Several fiber morphologies were found. Morphological evidence also indicated that a molten charged jet underwent the electrically-driven bending instability after it was ejected from the spinneret. The observed semi-angle of the cone at the critical point was about 37.5 ± 2^{o} compared to a 33.5^{o} predicted by Yarin and 49.9^{o} predicted by Taylor.

ACKNOWLEDGEMENT

This work was part of the first author's Ph.D. thesis and was done at the Maurice Morton Institute of Polymer Science, University of Akron, Akron, Oh, USA with a partial scholarship support from the Royal Thai Government.

REFERENCES

Chun, I. 1995. *Fine fibers spun by electrospinning process from polymer solutions and polymer melts in air and vacuum : characterization of structure and morphology on electrospun fibers and developing a new process model.* Doctoral Dissertation, The University of Akron, Akron, OH, USA.

Cross, J. A. 1987. *Electrostatics: Principles, Problems and Applications*. Bristol, Adam Hilger.

Doshi, J. 1994. *The electrospinning process and application of electrospun fibers.* Doctoral Dissertation, The University of Akron, Akron, OH, USA.

Doshi, J. and Reneker, D. H. 1993. *Proceeding of IEEE-Industry Applications Society, Annual Meeting, Toronto, Canada*. : 1698.

Koombhongse, S. 2001. *The formation of nanofibers from electrospinning process.* Doctoral Dissertation, The University of Akron, Akron, OH, USA.

Larrando, L. and Manley, R. ST. J. J. 1981. *J. Polym Sci., Part B: J. Polym Phys*. **19** : 909.

Lennhoff, J. D. *et al*. 2002. *The Fiber Society Fall Technical Meeting Book of Abstract-Presentation, October, Natick, MA* : 111.

Liu, W. *et al.* 2002. *The Fiber Society Fall Technical Meeting: Book of Abstracts - Poster, October, Natick, MA* : 43.

Rangkupan,R. 2002. *Electrospinning process of polymer melts*. Doctoral Dissertation, The University of Akron, Akron, OH, USA.

Schreuder-Gibson, H. and Gibson, P. 2002. *The Fiber Society Fall Technical Meeting: Book of Abstracts-Poster, October, Natick, MA* : 51.

Sigma-Aldrich. Milwaukee, WI. USA.

Taylor, G. I. 1964. *Proceedings of the Royal Society of London Series A*, **280** : 383.

Wang, X. *et al.* 2002. *The Fiber Society Fall Technical Meeting: Book of Abstract-Presentation, October, Natick, MA* : 118.

White, K. *et al*. 2002. *The Fiber Society Fall Technical Meeting Book of Abstract-Presentation, October, Natick, MA* : 127.

Yarin, A. L., Koombhongse, S. and Reneker, D. H. 2001. *J. Appl. Phys*. **90** : 4836.

(Revised version accepted April 1, 2003)